Published in final edited form as:
Eur J Neurosci. 2011 May ; 33(9): 1667–1676. doi:10.1111/j.1460-9568.2011.07652.x.

Terminal arbor degeneration (TAD): a novel lesion produced by the antineoplastic agent, paclitaxel

Gary J. Bennett[1,2,3], **Guo Kai Liu**[1,*], **Wen Hua Xiao**[1,2,*], **Hai Wei Jin**[1], and **Chiang Siau**[1]
[1]Department of Anesthesia, McGill University, Montréal, Québec, Canada
[2]The Alan Edwards Center for Research on Pain, McGill University, Montréal, Québec, Canada
[3]Faculty of Dentistry, McGill University, Montréal, Québec, Canada

Abstract

The anti-neoplastic agent, paclitaxel, causes a dose-limiting distal, symmetrical, sensory peripheral neuropathy that is often accompanied by a neuropathic pain syndrome. In a low-dose model of paclitaxel-evoked painful peripheral neuropathy in the rat, we have shown that the drug causes degeneration of intraepidermal nerve fibers (IENFs), i.e., the fibers which give rise to the sensory afferent's terminal receptor arbour. However, we did not find any evidence for axonal degeneration in samples taken at the mid-nerve level. Here we aimed to determine whether the absence of degenerating peripheral nerve axons was due to sampling a level that was too proximal. We used electron microscopy to study the distal-most branches of the nerves innervating the hind paw glabrous skin of normal and paclitaxel-treated rats. We confirmed that we sampled at a time when IENF degeneration was prominent. Because degeneration might be easier to detect with higher paclitaxel doses, we examined a four-fold cumulative dose range (8–32 mg/kg). We found no evidence of degeneration in the superficial subepidermal axon bundles (*s*SAB) that are located just a few microns below the epidermal basal lamina. Specifically, for all three dose groups there was no change in the number of *s*SAB per mm of epidermal border, no change in the number of axons per *s*SAB, and no change in the diameter of *s*SAB axons. We conclude that paclitaxel produces a novel type of lesion that is restricted to the afferent axon's terminal arbor; we name this lesion "terminal arbor degeneration (TAD)".

Keywords

chemotherapy neuropathy; intraepidermal nerve fiber; neuropathic pain; sensory neuropathy; rat; taxol

Introduction

Neurotoxicity is the dose-limiting side effect for the chemotherapeutic agent, paclitaxel. The toxicity presents as a chronic, distal, symmetrical, sensory peripheral neuropathy which is accompanied by a neuropathic pain syndrome in approximately 20% of patients receiving standard doses and nearly all patients receiving aggressive treatment. Sensory symptoms typically appear in the feet, or in the feet and hands, and are most pronounced in the sole and palm (Dougherty et al., 2004; Forsyth et al., 1997; Lipton et al., 1989; Wiernik et al., 1987). Peripheral neuropathy with similar or identical symptoms is also dose-limiting with other

Correspondence to: Gary J. Bennett, PhD, McGill University, 3655 Promenade Sir Wm. Osler, McIntyre Bldg., Room 1202, Montréal, Québec, Canada H3G 1Y6, gary.bennett@mcgill.ca; FAX : (514) 398-3432.
*These authors contributed equally to this work.

chemotherapeutics, including other taxanes and agents in the vinca alkaloid, platinum-complex, and proteasome-inhibitor classes (Cata et al., 2006; Quasthoff & Hartung, 2002; Verstappen et al., 2003; Windebank and Grisold, 2008).

We have produced paclitaxel-evoked painful peripheral neuropathy in the rat using a low-dose protocol: four injections of 2 mg/kg on alternate days; total dose: 8 mg/kg (Flatters & Bennett, 2004; Polomano et al., 2001). Electron microscopy studies with this model did not detect any sign of axonal degeneration in the saphenous nerve at a level just below the knee at the time of peak pain severity (Flatters & Bennett, 2006). Consistent with the absence of damage to peripheral nerve axons, we also found no up-regulation of activating transcription factor-3 (ATF-3), a marker of axonal injury (Tsujino et al., 2000), in the afferent neurons' nuclei (Flatters & Bennett, 2006). However, we subsequently found that the low-dose paclitaxel treatment causes a partial (ca. 25%) degeneration of intraepidermal nerve fibers (IENFs) in hind paw glabrous skin (Jin et al., 2008; Siau et al., 2006; Xiao et al., 2009). IENFs ramify within all the vital layers of the epidermis and issue multiple *en passant* and terminal varicosities (boutons). The IENF, its branches, and its receptor boutons constitute the sensory axon's terminal arbor (for reviews see (Kennedy & Wendelschafer-Crabb, 1993; Wang et al., 1990)).

The paradox of IENF loss without degeneration of peripheral nerve axons prompted the experiments reported here.

Materials and methods

All experimental protocols were approved by the Animal Care and Use Committee of the Faculty of Medicine, McGill University, in accordance with the regulations of the Canadian Council on Animal Care and the ethical guidelines of the Canadian Institutes of Health Research, the National Institutes of Health (USA), and the International Association for the Study of Pain (Zimmermann, 1983).

Study design

The aim was to determine whether our previous inability to find degenerating axons in the peripheral nerve (Flatters & Bennett, 2006) was due to sampling the nerve at a level that was too proximal, or whether it was due to the use of a borderline dose that produced only subtle degeneration. Thus we imaged the distal-most nerve branches that lie just below the epidermis and examined animals treated with our standard dose and animals receiving higher doses (24 and 32 mg/kg), where the highest dose approaches the LD_{50} with our dosing protocol. We confirmed that all three paclitaxel doses produced prominent IENF degeneration at the time of sampling. Lastly, because of the suspected link between axonal degeneration and paclitaxel-evoked neuropathic pain, we determined the time course of the behavioral effects of each of the three doses.

Animals

Adult male Sprague-Dawley rats (200–300g, Harlan Inc., Indianapolis, IN; Frederick, MD breeding colony) were housed on sawdust bedding in plastic cages. Artificial lighting was provided on a fixed 12 hour light-dark cycle with food and water available *ad libitum*.

Paclitaxel

Paclitaxel (Taxol®; Bristol-Myers-Squibb, 6mg/ml) was diluted with saline to a concentration of 2 mg/ml and injected IP. Rats received our standard dosing regimen (Flatters & Bennett, 2004, 2006; Polomano et al, 2001): 2 mg/kg on four alternate days (days 0 (D0), D2, D4 and D6); total dose: 8 mg/kg). Control animals were injected with 1

ml/kg of the vehicle. Separate groups were treated according to the same schedule but with four doses of 6 mg/kg (total dose: 24 mg/kg) or four doses of 8 mg/kg (total dose: 32 mg/kg.

IENF staining

As in our prior studies (Jin et al., 2008; Siau et al., 2006; Xiao et al., 2009), methods for IENF staining and quantification followed the clinical guidelines of the European Federation of Neurological Sciences (Lauria et al., 2005). We used a rabbit polyclonal IgG antibody raised against the conserved (rat, mouse, pig, human) residues 175–191 of the standard IENF marker, protein gene product 9.5 (PGP9.5; Research Diagnostics; Flanders, NJ; catalog number: RDI-PGP95MabR).

Following the induction of deep anesthesia via a sodium pentobarbital overdose (100 mg/kg; IP), the animals were perfused transcardially with a vascular rinse (0.1M phosphate buffered saline containing 0.05% sodium bicarbonate and 0.1% sodium nitrite) followed by freshly prepared 4% paraformaldehyde in 0.1M phosphate buffered saline, pH 7.4. The hind paws were severed and post-fixed overnight, after which a block of glabrous skin was excised from the wide part of the plantar hind paw that lies distal to the calcaneus and proximal to the digital tori. Blocks of skin were cryoprotected in 30% sucrose at 4°C overnight and then embedded in Optimal Cutting Temperature compound and stored at −80° C. Cryostat sections (30 μm) were collected in PBS and incubated for one hour in phosphate buffered saline containing 0.2% Triton-X 100 and 10% normal donkey serum (Jackson ImmunoResearch Laboratories; Mississauga, ON) at room temperature. Sections were then incubated in primary antibody diluted 1:6400 in phosphate buffered saline containing 0.2% Triton-X 100 and 5% normal donkey serum for 24 hr at 4°C. After rinsing, sections were incubated in donkey anti-rabbit IgG secondary antibody labeled with Cy3 (Jackson ImmunoReseach) diluted 1:200 for 1.5 hr. Control sections were prepared in the same way, but without incubation in primary antisera; no staining was seen in these sections.

IENF quantification

IENF counts were done by an observer blind as to the animal's group assignment. Using a 40X objective, all ascending nerve fibers that were seen to cross into the epidermis were counted; no minimum length was required, and fibers that branched within the epidermis were counted as one. A low magnification montage of each section (8–12 mm long) was made and the length of the epidermal border was measured. IENF counts are expressed as the number (mean ± SEM) per cm of epidermal border.

IENF time course

The time course of paclitaxel-evoked IENF degeneration was determined with our standard protocol (8 mg/kg total dose). We obtained tissue from paclitaxel-treated rats on D7, D14, D22, and D27 (n = 4/group) and compared these to a vehicle-injected control group (n = 4; one rat sacrificed at each time point). Skin samples were processed for the demonstration of IENFs as described above.

Effects of paclitaxel dose on IENF degeneration

We compared the amount of IENF loss in vehicle-treated animals and in animals receiving paclitaxel cumulative doses of 8 mg/kg, 24 mg/kg, and 32 mg/kg. The animals were sacrificed on D29–D36 (n = 4/group).

Effects of paclitaxel dose on ATF-3 staining

We have shown previously (Flatters and Bennett, 2006) that with our dosing protocol the 8 mg/kg cumulative dose of paclitaxel evokes IENF degeneration but does not evoke the

expression of ATF-3, a nuclear marker of axotomized neurons (Tsujino et al., 2000), in dorsal root ganglion (DRG) neurons. In order to determine whether the higher paclitaxel doses used here evoked this nerve-injury signal, we examined ATF-3 staining in rats that were treated with cumulative doses of 24 mg/kg and 32 mg/kg (n=4/group) and sacrificed on D30 (the approximate time of peak IENF loss). As a positive control we examined ATF-3 staining in the L4-L5 DRGs of two rats whose sciatic nerve had been transected three days before sacrifice.

The animals were prepared as described above and alternate 14 μm frozen sections were mounted onto slides and stained as described above. The anti-ATF-3 primary antibody (Santa-Cruz Biotechnology; Santa Cruz, CA; catalog number: sc-188 C-19; diluted 1:500) is an affinity purified, polyclonal IgG from rabbit immunized with a peptide corresponding to the protein's carboxy terminus, the sequence of which is identical in human and rat. The antibody has been used in numerous studies where its specificity has been confirmed by Western blotting, immunoprecipitation, and antigen pre-absorption (for review see (Starkey et al., 2009)). In the present experiments, we saw no ATF-3 staining in DRG neurons when sections were incubated without exposure to the primary antibody. Neuronal cell bodies were counter-stained with a fluorescent Nissl stain (Invitrogen; Carlsbad, CA; dilution: 1:300). We photographed 4–6 DRG sections from each rat and counted all cells that were sectioned through their nuclei and calculated the percentage that were AFT-3-positive.

Electron microscopy

Following the induction of deep anesthesia via a sodium pentobarbital overdose (100 mg/kg; IP), the animals were perfused transcardially with a vascular rinse (0.1M phosphate buffered saline containing 0.05% sodium bicarbonate and 0.1% sodium nitrite) followed by freshly prepared solution of 1% paraformaldehyde and 1% glutaraldehyde in 0.1M phosphate buffered saline, pH 7.4. Samples of glabrous hind paw skin was excised from the same location as that used for PGP9.5 immunocytochemistry, post-fixed for 3 h in the fixative described above, transferred to 10% sucrose in 0.1 M phosphate buffered saline and kept at 4° C for 12 h. The samples were then incubated in 1% osmium tetroxide in 0.1 M phosphate buffered saline, pH 7.4, at 4° C for 2 h, dehydrated in ascending concentrations of alcohol and propylene oxide at room temperature, and embedded in Epon. Ultrathin sections were acquired with a microtome using a diamond knife, collected on Formvar-coated grids, and counterstained with lead citrate and uranyl acetate. Grids were observed in a Philips EM410 electron microscope operated at 80 kV. Photomicrographs were taken and analyzed using a Megaview II CCD camera and AnalySIS 5.0 software (both from Soft Imaging System Corp., Lakewood, CO).

We examined 8 mg/kg, 24 mg/kg and 32 mg/kg paclitaxel-treated animals and vehicle-treated controls (n = 4/group). The animals were sacrificed at the time of confirmed IENF loss (D29–D36). Electron photomicrographs of subepidermal axon bundles (see below) were taken at 15,000X. Axon diameters were calculated as the mean of the longest and shortest orthogonal diameters for all profiles cut in approximate cross section (longest/shortest diameter ratios ≤ 2.0). A montage of the entire section was created from low magnification (135X) photomicrographs and used to measure the length (straight line approximation) of the dermal-epidermal border. One section was examined in its entirety for each rat.

Behavioral testing

Animals (n = 6–8/group) were habituated to the behavioral testing environment and three baseline measurements of mechanical sensitivity were taken prior to drug administration. The animals were placed on an elevated wire mesh floor and confined beneath overturned mouse cages made of clear plastic. von Frey filaments with bending forces of 4g and 15g

were applied to the mid-plantar skin (avoiding the base of the tori) of each hind paw 5 times, with each application held for 5 seconds. Withdrawal responses to the von Frey filaments from both hind paws were counted and then expressed as an overall percentage response. Normal rats rarely withdraw from the 4g stimulus; the increased level of responding seen after drug treatment is thus indicative of mechano-allodynia. Normal animals withdraw from the 15g stimulus 10–20% of the time; the increased level of responding seen after treatment is thus indicative of mechano-hyperalgesia. Heat-hyperalgesia was not tested as our paclitaxel model produces little or no change in sensitivity to noxious heat (Polomano et al., 2001).

Statistical analyses

Results were analyzed with the GraphPad InStat program (GraphPad Software, Inc.; La Jolla, CA). One-way ANOVAs followed by Dunnett's *t*-test comparisons to the control group were used to analyze (1) the IENF degeneration time course data, and (2) the data from the subepidermal axon bundle measurements (number of bundles per mm epidermal border, number of axons per bundle, and axon diameters). The effects of paclitaxel dose on IENF degeneration were analyzed with unpaired *t*-test comparisons to each group's vehicle-injected control group. The behavioral time course data for mechano-allodynia and mechano-hyperalgesia were analyzed with repeated-measures ANOVA for each group followed by Dunnett's *t*-test comparisons to each group's pre-injection baseline scores.

Results

All rats receiving 8 mg/kg, 24 mg/kg, or 32 mg/kg cumulative doses of paclitaxel appeared to be healthy except for cessation of weight gain during the treatment period; weight gain resumed post-treatment. In a pilot study we found that a cumulative dose of 48 mg/kg (4 × 12 mg/kg) produced 50% mortality.

Effects of paclitaxel dose on ATF-3 staining

In the rats with sciatic nerve transection, 50% of DRG cells were ATF-3-positive (1686/3344 cells). This is the expected outcome as it is known that approximately one-half of the L4/L5 DRG neurons have their axons in the sciatic nerve in the rat (Devor et al., 1985). There were no ATF-3-positive DRG neurons in any of the rats treated with 24 and 32 mg/kg paclitaxel (24 mg/kg: 0/4648 cells; 32 mg/kg: 0/4639 cells).

IENF degeneration time course

Paclitaxel treatment caused a statistically significant loss of IENFs ($F_{4,15} = 4.00$, $p = 0.02$). Vehicle-injected control animals had (mean ± SEM) 365.8 ± 51.6 IENFs per cm of epidermal border (Fig. 1). There was no change on D7 (363.8 ± 18.9 IENFs per cm). There was a statistically non-significant decrease of −17.1 ± 3.9% (303.3 ± 14.2 IENF/cm) on D14 and statistically significant decreases of −20.5 ± 3.0% (290.8 ± 10.9 IENF/cm) on D22 and −20.5 ± 5.3% (290.8 ± 19.5 IENFs/cm) on D27.

Effects of paclitaxel dose on IENF degeneration

All three paclitaxel doses produced a statistically significant loss of IENFs. Animals in the vehicle-treated control group had 339.8 ± 13.7 IENFs per cm of epidermal border. Rats receiving 8 mg/kg, 24 mg/kg or 32 mg/kg paclitaxel had statistically significant decreases of −20.7 ± 3.6% ($t_6 = 2.56$, $p = 0.021$), −28.6 ± 9.0% ($t_6 = 3.11$, $p = 0.011$), and −39.4 ± 8.5% ($t_6 = 3.87$, $p = 0.004$), respectively (Fig. 2).

Electron microscopy

We found small bundles of axons located a few microns below the basal lamina that separates the epidermis and the dermis. (Figs. 3, 4, and 5). These subepidermal axon bundles (SAB) consisted of small (mean diameter: 0.45 μm) unmyelinated axonal profiles enveloped by a non-myelinating Schwann cell (SC) and its basal lamina. We refer to these structures as "bundles" to distinguish them from nerves and nerve fascicles which, by definition, are surrounded by an epineurium and/or perineurium. We identified two types of SAB: superficial (*s*SAB) and deep (*d*SAB).

The *s*SAB was found within indentations in the dermal-epidermal border (Figs. 3, 4 and 5B) or in a region immediately subjacent to such indentations. The indentations were located beneath the junction between keratinocytes. We never saw an *s*SAB (n = 376) with the SC's nucleus present and it is thus possible that the *s*SAB's SC process originates from the SC that surrounds its parent *d*SAB (see below). There was a notable widening of the mesaxon of axons situated along the periphery of an *s*SAB; presumably reflecting the fact that axon is preparing to leave the bundle (Figs. 4 and 5C).

The *d*SAB were found at or just below the monolayer of papillary fibroblasts (Sorrell & Caplan, 2004) that lays a few microns below the epidermal basal lamina (Figs. 3 and 5A). We did not find any *d*SAB (n = 243) with multiple SC nuclei and thus presume that each bundle consists of a single Schwann cell and its processes. A *d*SAB contained an average of 18.7 axons, which is about 3 times as many axons as an average *s*SAB (6.8 axons). It is thus likely that a *d*SAB gives rise to multiple *s*SAB. The axons within *d*SAB were all small and most had pale, often watery, axoplasm with few or no neurofilaments; they were similar in all respects to the axons seen within *s*SABs. It is known that as nerve fascicles approach the epidermis they loose their epineurium and are wrapped with multiple layers of perineurial cells. The thickness of the perineurial sheath decreases gradually via the progressive loss of the innermost cells and the distal-most nerve fascicles are wrapped in a single perineurial cell (Breathnach, 1977; Coërs, 1982). It must be that *d*SAB arise via the loss of the last perineurial cell.

Paclitaxel effects on *SAB*

We saw no evidence of degenerating axons in the *s*SAB or *d*SAB in any of the paclitaxel-treated rats. Pale and sometimes watery axoplasm with few or no neurofilaments is characteristic of peripheral nerve axons undergoing degeneration. However, pale axoplasm without neurofilaments was observed in many axons in the *s*SAB and *d*SAB of normal rats, and the appearance of the axoplasm in all three paclitaxel groups was indistinguishable from normal. Others have noted that IENFs also often have pale axoplasm with few or no neurofilaments (Lauria et al., 2004).

Our quantification focused on *s*SAB axons as this is the most distal level prior to the emergence of the IENFs. We examined a total of 376 SABs that contained a total of 2550 axons. None of the three paclitaxel doses had any effect on SABs.

Control animals had 17.0 ± 2.6 *s*SAB per mm of dermal-epidermal border (Fig. 6A). Animals receiving 8 mg/kg, 24 mg/kg or 32 mg/kg paclitaxel had 20.7 ± 2.4, 17.0 ± 3.8, and 19.1 ± 2.0 *s*SAB per mm of border, respectively. There are no statistically significant differences between groups ($F_{3,11} = 0.40$, p = ns).

Control animals had 6.7 ± 0.5 axons per *s*SAB (Fig. 6B). Animals receiving 8 mg/kg, 24 mg/kg or 32 mg/kg paclitaxel had 7.0 ± 0.3, 6.6 ± 0.5, and 6.5 ± 0.9 axons per *s*SAB, respectively. There are no statistically significant differences between groups ($F_{3,11} = 0.20$, p = ns).

We computed the diameter of all axons that had long vs. short diameter rations ≤ 2.0 (Fig. 6C). The average diameter of *s*SAB axons in the control group was 0.451 ± 0.095 μm (n = 611). The average axonal diameters in the 8 mg/kg, 24 mg/kg or 32 mg/kg paclitaxel groups were 0.415 ± 0.055 μm (n = 840), 0.477 ± 0.068 μm (n = 672), and 0.447 ± 0.022 μm (n = 427), respectively. There are no statistically significant differences between groups ($F_{3,11}$ = 0.17, p = ns). There were no outlier values (atypically small or large diameters) in any of the three dosage groups, i.e., the paclitaxel groups did not contain shrunken or swollen axons.

Neuropathic pain

As shown in Fig. 7, all three doses of paclitaxel produced statistically significant mechano-allodynia and mechano-hyperalgesia. As expected from our prior studies (Flatters & Bennett, 2004,2006;Polomano et al., 2001), rats treated with 8 mg/kg paclitaxel developed statistically significant mechano-allodynia ($F_{7,72}$ = 10.91, p < 0.0001) and mechano-hyperalgesia ($F_{7,88}$ = 21.10, p < 0.0001) starting 10 days after the last dose of paclitaxel. Rats receiving 24 mg/kg developed statistically significant mechano-allodynia ($F_{8,40}$ = 19.40, p < 0.0001) and mechano-hyperalgesia ($F_{8,40}$ = 14.98, p < 0.0001) starting on D12 (6 days after the last paclitaxel injection). Rats receiving 32 mg/kg developed statistically significant mechano-allodynia ($F_{7,49}$ = 12.69, p < 0.0001) and mechano-hyperalgesia ($F_{7,49}$ = 13.95, p < 0.0001) starting on D10 (4 days after the last injection). Notably, all three dosage groups reached approximately the same peak severity of mechano-allodynia and mechano-hyperalgesia by D26–D30.

Discussion

TAD (terminal arbor degeneration) is a novel neural lesion

We examined the effects of a four-fold dose range of paclitaxel. With our dosing schedule, the lowest cumulative dose (8 mg/kg) is close to the threshold amount needed to produce the neuropathic pain syndrome (Polomano et al., 2001), while the highest exposure (32 mg/kg) is close to a lethal dose (LD_{50}: 48 mg/kg). None of the doses produce the ATF-3 signal in DRG neurons. We confirmed that samples for electron microscopy were obtained at a time at which all three dose groups had prominent IENF degeneration (20–40%). It is noteworthy that none of the groups had any sign of axonal degeneration below the epidermal basal lamina. We conclude that within this dose range, paclitaxel-evoked degeneration is confined to the IENFs, i.e., the sensory fibers' intraepidermal terminal arbors. To our knowledge, this type of neural lesion has not been described previously; we propose to call it "terminal arbor degeneration (TAD)".

We have considered three alternative interpretations of our data. First, our conclusion is based on the premise that all IENFs are derived from an *s*SAB. We think this is correct because in the regions above and below the fibroblast layer we never observed any axons (myelinated or unmyelinated) that were not within an *s*SAB or *d*SAB. Thus, we have no reason to doubt that *s*SABs are the source of all IENFs. Motor neuron axons are known to leave nerve fascicles and approach muscle fibers as isolated axons (Burkel, 1967), but we are not aware of any report showing that this happens for sensory axons entering the epidermis.

Second, IENF loss was identified immunocytochemically while SAB axons were identified morphologically. Thus, there is the possibility that the IENF loss may not be due to degeneration but rather to a paclitaxel-evoked down-regulation of the demonstrated antigen. This is an unlikely possibility. The PGP9.5 antibody recognizes a house-keeping enzyme, ubiquitin C-terminal hydrolase (Wilkinson et al., 1989), which is expressed at very similar levels by all the afferent cell bodies in the DRG (Calzada et al., 1994). There is no evidence

to show that PGP9.5 is absent from some IENFs and there is no evidence that this enzyme is down-regulated after neuronal insult. In fact, IENFs are PGP9.5-positive even when they have begun to degenerate following nerve transection and acrylamide poisoning (Ebenezer et al., 2007; Hseih et al., 2000; Ko et al., 2000; Lauria et al., 2004).

Third, there is the question of whether TAD is a distinct lesion, or merely the initial manifestation of a progressive dying-back process. Three lines of evidence indicate that TAD is distinct. (1) If paclitaxel evoked progressive die-back, then one might miss seeing degeneration if the sample was obtained during an early stage of the process, or if the sample was obtained from a location that was proximal to the level where degeneration was present. But we obtained samples at a time of advanced IENF loss and the level that we examined was just a few tens of microns from the axon's termination. (2) SAB axons in the process of degeneration might be expected to be swollen or shrunken. However, we found no difference in the diameters of *s*SAB axons for any of the dose groups. (3) If TAD were the initial sign of a progressive dying-back process, then one would expect to see at least some indication of degeneration beneath the epidermis, particularly with the highest dose of paclitaxel that produced a 40% loss of IENFs. We found no evidence of degeneration with any of the doses.

Lastly, we note that it is not correct to say that paclitaxel-evoked peripheral neuropathy resembles the progressive, distal, symmetrical, dying-back type of peripheral neuropathy seen in diabetes. It is true that both are distal and symmetrical, but there is reason to doubt that paclitaxel-evoked neuropathy is progressive. Diabetic peripheral neuropathy is clearly a progressive process -- sensory deficits and pain begin at the toes, slowly spread up the feet and legs, then appear in the fingers and spread into the rest of the hand and into the forearm, and finally appear in the ventral midline of the trunk (Neundörfer & Thomas, 2003). In contrast, paclitaxel patients sometimes report the simultaneous (or nearly simultaneous) onset of symptoms in the feet and the hands, and cases have been reported where symptoms appear in the hands before the feet (Forsyth et al., 1997; Lipton et al., 1989). The simultaneous appearance of symptoms in the hands and feet is not congruent with a progressive dying-back phenomenon.

Multiple mechanisms of paclitaxel neurotoxicity?

Our standard low-dose model (4 injections of 2 mg/kg) does not produce axonal degeneration at the peripheral nerve level, does not produce ATF-3 up-regulation in DRG neurons, and did not produce any degeneration of SAB axons. Four injections of 6 mg/kg or 8 mg/kg also did not cause degeneration of SAB axons or ATF-3 up-regulation.

However, other studies in the rat that used a higher single dose intensity (12.5–32 mg/kg: Authier et al., 2000; Cliffer et al., 1998; Jamieson et al., 2007; Jimenz-Andrade et al., 2006; Peters et al., 2007a,b) or a higher cumulative dose (40–80 mg/kg: (Cavaletti et al., 1995; Persohn et al., 2005) have found degeneration of axons in the peripheral nerve and dorsal root, and ATF-3 up-regulation in DRG neurons. We are aware of only two paclitaxel-treated patients whose peripheral nerves have been examined microscopically. The nerve of one patient was unremarkable (Wiernik et al., 1987) but the sural nerve biopsy from the other patient showed extensive axonal degeneration (Sahenk et al., 1994). However, this patient had been treated previously with cisplatin (which also produces peripheral neuropathy) and had received 17 courses of treatment with a high dose of paclitaxel (275 mg/m^2), resulting in an extraordinary cumulative dose of 6,603 mg/m^2. Thus, one can conclude that in the rat high doses of paclitaxel can produce degeneration of peripheral nerve sensory axons and can kill their cell bodies in the DRG, and that this may occur in at least some patients.

This suggests that paclitaxel-evoked neurotoxicity potentially involves at least two pathological mechanisms, one with a low-dose threshold that produces TAD, and another with a higher-dose threshold that causes degeneration of peripheral nerve axons and ATF-3 up-regulation (and perhaps a third mechanism with a still higher threshold that kills the neuronal cell body). There is evidence that different neuronal compartments (cell bodies, axons, and synaptic boutons) have distinctly different mechanisms of degeneration (Gillingwater & Ribchester, 2003; Ikegami & Koike, 2003; Raff et al., 2002; Wang et al., 2002) and that these compartment-specific mechanisms are engaged at different threshold levels of exposure to toxins (LoPachin, 2005; Melli et al., 2006; Silva et al., 2006). We propose that the terminal arbor of sensory afferent neurons is another such compartment.

Subepidermal axon bundles

The SAB has not been well described in prior investigations. They have been mentioned briefly in ultrastructural studies of adult human skin (Cauna, 1968; Orfanos & Mahrle, 1973) and a photomicrograph of what may be a developmental precursor of an SAB appears in a study of human fetal skin (Breathnach, 1977). Ebenezer et al. (2007) show "Remak bundles" in the superficial dermis of adult human skin and these are probably identical to the *d*SAB described here. We think it is important to distinguish SABs from Remak bundles. Remak bundles in nerves contain only unmyelinated C-fibers. In contrast, at least some SAB must contain the pre-terminal, unmyelinated portions of A-fibers that have lost their myelin sheaths. This is particularly noteworthy for the intraepidermal myelinated nociceptors, which have parent axons conducting in both the Aδand Aβ ranges (Djouhri & Lawson, 2004).

Why is the lesion specific for the sensory afferent axon's terminal receptor arbor?

High levels of paclitaxel are found in the DRG, but not in peripheral nerve or spinal cord (Cavaletti et al., 2000). Thus the primary afferent cell bodies are exposed to a high level of paclitaxel, but the motor neuron cell bodies are not. Paclitaxel levels in IENFs are not known, but may be higher than in peripheral nerve because the SABs lack perineurium (a component of the blood-nerve barrier). It may be that IENFs are exposed to paclitaxel via anterograde transport from the cell body. It would take time for such anterogradely transported paclitaxel to accumulate to injurious levels in the terminal arbors. This accumulation time might correspond to the coasting effect, i.e., the delay between treatment cessation and the loss of IENFs and the appearance of pain hypersensitivity.

We have hypothesized that paclitaxel-evoked neuropathy is due to a metabolic insult - a toxic effect on axonal mitochondria that impairs the axon's energy supply (Jin et al., 2008; Flatters & Bennett, 2006; Flatters et al., 2006; Siau & Bennett, 2006; Siau et al., 2006; Xiao & Bennett, 2008; Xiao et al., 2009). Recent work has confirmed the presence of defects in mitochondrial respiratory complexes I and II in peripheral nerve from rats with paclitaxel-evoked (and oxaliplatin-evoked) painful peripheral neuropathy (Zheng et al., 2010).

If severe enough, energy deficiency will produce degeneration, and the threshold for degeneration will be lowest in the neuronal compartment that has the highest energy requirement. We propose that the sensory axon's terminal receptor arbor is the compartment with the highest energy requirement. Mitochondria are known to concentrate in regions of high metabolic demand (Chen & Chan, 2006; Mironov, 2007) and sensory terminal boutons are packed with mitochondria. This has been documented in intraepidermal receptor boutons (Breathnach 1977; Cauna, 1968; Orfanos & Mahrle, 1973; Ribeiro-da-Silva et al., 1991; Winklemann, 1967), including the boutons of physiologically identified A-fiber nociceptors (Kruger et al., 1981).

We propose that the intraepidermal terminal arbor's high energy requirement is due, at least in part, to a unique phenomenon – the arbor is in a constant process of alternating degeneration and regeneration (re-modeling) due to its constantly changing microenvironment. The epidermis renews itself continuously. This occurs at a fairly high rate; in man under basal conditions, it takes about 14 days for a newly generated keratinocyte to travel from the stratum basales to the bottom of the stratum corneum (Bergstresser & Taylor, 1977). As keratinocytes are displaced upwards by newly generated cells, they loose their cubiodal shape and become progressively flattened. Importantly, this movement and change in cell shape must alter the geometry of the very complex spaces between adjacent keratinocytes. Junctions between keratinocytes are characterized by finger-like processes from each cell that interdigitate and are periodically cemented together by desmosomes (Montagna, 1962). The IENF and its branches travel in the junctions between keratinocytes and must accommodate to the junctions' constantly changing geometry.

Two lines of evidence support this idea. First, growth-associated protein 43 (GAP43) is generally present only in neurons that are regenerating after injury. But GAP43-positive IENFs are a consistent finding in normal skin in man, rat and mouse (for reviews see Verzé et al. (2003a, b)). About 40% of IENFs are GAP43-positive in the plantar hind paw of the normal mouse (Beiswenger et al., 2008). Second, IENFs sometimes bear vacuolated, round or oval swellings with diameters that are two or more times greater than the parent fiber's diameter (and hence distinct from the smaller *en passant* and terminal boutons) (Hermann et al., 2004; Wendelschafer-Crabb et al., 2006). In animals, the incidence of these swellings is greatly increased just prior to degeneration due to nerve transection or acrylamide poisoning (Hseih et al., 2000; Ko et al., 2000). The incidence of swellings is also increased in patients with peripheral neuropathies (Ebenezer et al., 2007; Hermann et al., 2004; Lauria et al., 2003; Wendelschafer-Crabb et al., 2006). Thus IENF swellings have been thought to reflect early degenerative changes that predict IENF loss. However, all of the studies noted above have found a relatively high incidence of IENF swellings in normal skin. This is explicable if swellings are indeed associated with degeneration and if an ongoing process of degeneration/regeneration (re-modeling) is normally present. The presence of a normal ongoing process of degeneration/regeneration is also a likely explanation for why IENF degeneration does not evoke the ATF-3 injury response in the DRG.

TAD and other peripheral neuropathies

TAD may be a common lesion in toxic neuropathies. In rats, the cancer chemotherapeutics, vincristine and oxaliplatin, produce a neuropathic pain syndrome with IENF degeneration but without degeneration of peripheral nerve axons (Aley et al., 1996; Siau et al., 2006; Tanner et al, 1998; Topp et al., 2000; Wallace et al., 2007; Xiao & Bennett, 2010). Clinically, IENF loss has been found in peripheral neuropathy patients who had normal nerve conduction studies (Devigili et al., 2008; Løseth et al., 2008; Periquet et al., 199l) and normal peripheral nerve axon counts (Hermann et al., 1999; Holland et al., 1998). The observation of IENF loss in conjunction with normal axon counts in the peripheral nerve led Holland et al. (1998) to propose the possibility of "terminal axonopathy", an idea that is close to the TAD concept.

TAD and neuropathic pain

With the 8 mg/kg dose, there is a correspondence between the onset of TAD and the onset of paclitaxel-evoked mechano-allodynia and mechano-hyperalgesia -- both appear after a delay of about two weeks from the last injection of paclitaxel. We have found the same delay to onset for paclitaxel-evoked cold-allodynia (Flatters & Bennett, 2004). A similar delay, called "coasting", is seen clinically when chemotherapy-evoked peripheral neuropathy

continues to worsen or appears initially in the period between treatment cycles (Cata et al., 2006; Quasthoff & Hartung, 2002; Verstappen et al., 2003; Windebank & Grisold, 2008). Coasting is consistent with the idea that accumulating toxicity must pass a threshold level before the appearance of symptoms. The shorter delays in pain onset seen with the 24 mg/kg and 32 mg/kg doses are consistent with this idea. It is of importance to note that paclitaxel-evoked neuropathic pain is not associated with the degeneration of peripheral nerve axons; the TAD lesion alone, or some phenomenon related to it, is sufficient to produce neuropathic pain.

Acknowledgments

This work was supported by research grants to GJB from the National Institute of Neurological Disorders and Stroke, National Institutes of Health, U.S.A. [R01-NS052255], the Neuropathy Association, and the Canada Research Chairs Program. GKL was a Postdoctoral Research Fellow of the Canada Research Chairs Program. HWJ was a Ronald Melzack Postdoctoral Research Fellow of the Louise and Alan Edwards Foundation of Montreal. CS was a Research Fellow of the A*STAR Program of Singapore. GJB is a Canada Senior Research Chair.

Abbreviations

ATF-3	activating transcription factor-3
DRG	dorsal root ganglion
IENF	intraepidermal nerve fiber
SAB	subepidermal axon bundle
***s*SAB**	SAB superficial to the papillary fibroblast layer
***d*SAB**	SAB deep to the papillary fibroblast layer
PGP9.5	protein gene product 9.5
TAD	terminal arbor degeneration

References

Aley KO, Reichling DB, Levine JD. Vincristine hyperalgesia in the rat: a model of painful vincristine neuropathy in humans. Neuroscience. 1996; 73:259–265. [PubMed: 8783247]

Authier N, Gillet JP, Fialip J, Eschalier A, Coudore F. Description of a short-term Taxol-induced nociceptive neuropathy in rats. Brain Res. 2000; 887:239–249. [PubMed: 11134612]

Beiswenger KK, Calcutt NA, Mizisin AP. Dissociation of thermal hypoalgesia and epidermal denervation in streptozotocin-diabetic mice. Neurosci. Lett. 2008; 442:267–272. [PubMed: 18619518]

Bergstresser PR, Taylor JR. Epidermal “turnover-time” - a new examination. Br. J. Dermatol. 1997; 96:503–509. [PubMed: 871385]

Breathnach AS. Electron microscopy of cutaneous nerves and receptors. J. Invest. Dermatol. 1977; 69:8–26. [PubMed: 326994]

Burkel WE. The histological fine structure of perineurium. Anat. Rec. 1967; 158:177–190. [PubMed: 6039587]

Calzada B, Naves FJ, Del Valle ME, Vega JA. Distribution of protein gene product 9.5 (PGP 9.5) immunoreactivity in the dorsal root ganglia of adult rat. Ann. Anat. 1994; 176:437–441. [PubMed: 7978340]

Cauna, N. Light and electron microscopical structure of sensory end-organs in human skin. In: Kenshalo, DR., editor. The Skin Senses. Springfield IL: CC Thomas; 1968. p. 15-37.

Cavaletti G, Tredici G, Braga M, Tazzari S. Experimental peripheral neuropathy induced in adult rats by repeated intraperitoneal administration of taxol. Exp. Neurol. 1995; 133:64–72. [PubMed: 7601264]

Cavaletti G, Cavalletti E, Oggioni N, Sottani C, Minoia C, D'Incalci M, Zucchetti M, Marmiroli P, Tredici G. Distribution of paclitaxel within the nervous system of the rat after repeated intravenous administration. Neurotoxicology. 2000; 21:389–3893. [PubMed: 10894128]

Cata JP, Weng HR, Lee BN, Reubgen JM, Dougherty PM. Clinical and experimental findings in humans and animals with chemotherapy-induced peripheral neuropathy. Minerva Anestesiol. 2006; 72:151–169. [PubMed: 16493391]

Chen H, Chan DC. Critical dependence of neurons on mitochondrial dynamics. Curr. Opin. Cell Biol. 2006; 18:453–459. [PubMed: 16781135]

Cliffer KD, Siuciak JA, Carson SR, Radley HE, Park JS, Lewis DR, Zlotchenko E, Nguyen T, Garcia K, Tonra JR, Stambler N, Cedarbaum JM, Bodine SC, Lindsay RM, DiStefano PS. Physiological characterization of Taxol-induced large-fiber sensory neuropathy in the rat. Ann. Neurol. 1998; 43:46–55. [PubMed: 9450768]

Coërs, C. Motor and sensory endings in skeletal muscle: histology. In: Haymaker, W.; Adams, RD., editors. Histology and Histopathology of the Nervous System. Springfield IL: CC Thomas; 1982. p. 1616-1622.

Devigili G, Tugnoli V, Penza P, Camozzi F, Lombardi R, Melli G, Broglio L, Granieri E, Lauria G. The diagnostic criteria for small fibre neuropathy: from symptoms to neuropathology. Brain. 2008; 131:1912–1925. [PubMed: 18524793]

Devor M, Govrin-Lippmann R, Frank I, Raber P. Proliferation of primary sensory neurons in adult rat dorsal root ganglion and the kinetics of retrograde cell loss after sciatic nerve section. Somatosens Res. 1985; 3:139–167. [PubMed: 3835669]

Djouhri L, Lawson SN. A-beta-fiber nociceptive primary afferent neurons: a review of incidence and properties in relation to other afferent A-fiber neurons in mammals. Brain Res. Rev. 2004; 46:131–145. [PubMed: 15464202]

Dougherty PM, Cata JP, Cordella JV, Burton A, Weng HR. Taxol-induced sensory disturbance is characterized by preferential impairment of myelinated fiber function in cancer patients. Pain. 2004; 109:132–142. [PubMed: 15082135]

Ebenezer GJ, McArthur JC, Thomas D, Murinson B, Hauer P, Polydefkis M, Griffin JW. Denervation of skin in neuropathies: the sequence of axonal and Schwann cell changes in skin biopsies. Brain. 2007; 130:2703–2714. [PubMed: 17898011]

Flatters SJL, Bennett GJ. Ethosuximide reverses paclitaxel- and vincristine-induced painful peripheral neuropathy. Pain. 2004; 109:50–61.

Flatters SJL, Bennett GJ. Studies of peripheral sensory nerves in paclitaxel-induced painful peripheral neuropathy: Evidence for mitochondrial dysfunction. Pain. 2006; 122:247–257.

Flatters SJL, Xiao WH, Bennett GJ. Acetyl-L-carnitine prevents and reduces paclitaxel-induced painful neuropathy. Neurosci. Lett. 2006; 397:219–223. [PubMed: 16406309]

Forsyth PA, Balmaceda C, Peterson K, Seidman AD, Brasher P, DeAngelis LM. Prospective study of paclitaxel-induced peripheral neuropathy with quantitative sensory testing. J. Neurooncol. 1997; 35:47–53. [PubMed: 9266440]

Gillingwater TH, Ribchester RR. The relationship of neuromuscular synapse elimination to synaptic degeneration and pathology: insights from Wld^S and other mutant mice. J. Neurocytol. 2003; 32:863–881. [PubMed: 15034273]

Herrmann DN, Griffin JW, Hauer P, Cornblath DR, McArthur JC. Epidermal nerve fiber density and sural nerve morphometry in peripheral neuropathies. Neurology. 1999; 53:1634–1640. [PubMed: 10563605]

Hermann NR, McDerott MP, Henderson D, Chen L, Akowuah K, Schifitto G. North East AIDS Dementia (NEAD) Consortium. Epidermal nerve fiber density, axonal swellings and QST as predictors of HIV distal sensory neuropathy. Muscle Nerve. 2004; 29:420–427. [PubMed: 14981742]

Holland NR, Crawford TO, Hauer P, Cornblath DR, Griffin JW, McArthur JC. Small fiber sensory neuropathies: clinical course and neuropathology of idiopathic cases. Ann. Neurol. 2008; 44:47–59. [PubMed: 9667592]

Hsieh ST, Chiang HY, Lin WM. Pathology of nerve terminal degeneration in the skin. J. Neuropathol. Exp. Neurol. 2000; 59:297–307. [PubMed: 10759185]

Ikegami K, Koike T. Non-apoptotic neurite degeneration in apoptotic neuronal death: pivotal role of mitochondrial function in neurites. Neuroscience. 2003; 122:617–626. [PubMed: 14622905]

Jamieson SM, Liu JJ, Connor B, Dragunow M, McKeage MJ. Nucleolar enlargement, nuclear eccentricity and altered cell body immunostaining characteristics of large-sized sensory neurons following treatment of rats with paclitaxel. Neurotoxicology. 2007; 28:1092–1098. [PubMed: 17686523]

Jimenez-Andrade JM, Peters CM, Mejia NA, Ghilardi JR, Kuskowski MA, Mantyh PW. Sensory neurons and their supporting cells located in the trigeminal, thoracic and lumbar ganglia differentially express markers of injury following intravenous administration of paclitaxel in the rat. Neurosci. Lett. 2006; 405:62–67. [PubMed: 16854522]

Jin HW, Flatters SJL, Xiao WH, Mulhern HL, Bennett GJ. Prevention of paclitaxel-evoked painful peripheral neuropathy by acetyl-L-carnitine: Effects on axonal mitochondria, sensory nerve fiber terminal arbors, and cutaneous Langerhans cells. Exptl. Neurol. 2008; 210:229–237. [PubMed: 18078936]

Kennedy WR, Wendelschafer-Crabb G. The innervation of human epidermis. J. Neurol. Sci. 1993; 115:184–190. [PubMed: 8482979]

Ko MH, Chen WP, Hsieh ST. Cutaneous nerve degeneration induced by acrylamide in mice. Neurosci. Lett. 2000; 293:195–198. [PubMed: 11036194]

Kruger L, Perl ER, Sedivec MJ. Fine structure of myelinated mechanical nociceptor endings in cat hairy skin. J. Comp. Neurol. 1981; 198:137–154. [PubMed: 7229137]

Lauria G, Morbin M, Lombardi R, Borgna M, Mazzoleni G, Sghirlanzoni A, Pareyson D. Axonal swellings predict the degeneration of epidermal nerve fibers in painful neuropathies. Neurology. 2003; 61:631–636. [PubMed: 12963753]

Lauria G, Borgna M, Morbin M, Lombardi R, Mazzoleni G, Sghirlanzoni A, Pareyson D. Tubule and neurofilament immunoreactivity in human hairy skin: markers for intraepidermal nerve fibers. Muscle Nerve. 2004; 30:310–316. [PubMed: 15318342]

Lauria G, Cornblath DR, Johansson O, McArthur JC, Mellgren SI, Nolano M, Rosenberg N, Sommer C. European Federation of Neurological Societies. EFNS guidelines on the use of skin biopsy in the diagnosis of peripheral neuropathy. Eur. J. Neurol. 2005; 12:747–758. [PubMed: 16190912]

Lipton RB, Apfel SC, Dutcher JP, Rosenberg R, Kaplan J, Berger A, Einzig AI, Wiernik P, Schaumburg HH. Taxol produces a predominantly sensory neuropathy. Neurology. 1989; 39:368–373. [PubMed: 2564647]

Løseth S, Stålberg E, Jorde R, Mellgren SI. Early diabetic neuropathy: thermal thresholds and intraepidermal nerve fibre density in patients with normal nerve conduction studies. J. Neurol. 2008; 255:1197–1202. [PubMed: 18574618]

LoPachin RM. Acrylamide neurotoxicity: neurological, morphological and molecular endpoints in animal models. Adv. Exp. Med. Biol. 2005; 561:21–37. [PubMed: 16438286]

Melli G, Keswani SC, Fischer A, Chen W, Höke A. Spatially distinct and functionally independent mechanisms of axonal degeneration in a model of HIV-associated sensory neuropathy. Brain. 2006; 129:1330–1338. [PubMed: 16537566]

Mironov SL. ADP regulates movements of mitochondria in neurons. Biophys. J. 2007; 92:2944–2952. [PubMed: 17277190]

Montagna, W. The Structure and Function of Skin. New York: Academic Press; 1962. p. 14

Navarro N, Verdu E, Wendelschafer-Crabb G, Kennedy WR. Innervation of the cutaneous structures in the mouse hind paw: A confocal microscopy immunohistochemical study. J. Neurosci. Res. 1995; 41:111–120. [PubMed: 7545760]

Neundörfer, B.; Thomas, PK. Diabetic sensorimotor neuropathy: clinical features. In: Gries, FA.; Cameron, NE.; Low, PA.; Ziegler, D., editors. Textbook of Diabetic Neuropathy. Stuttgart: Thieme; 2003. p. 199-204.

Orfanos CE, Mahrle G. Ultrastructure and cytochemistry of human cutaneous nerves. J. Invest. Dermatol. 1973; 61:108–120. [PubMed: 4125554]

Periquet MI, Novak V, Collins MP, Nagaraja HN, Erdem S, Nash SM, Freimer ML, Sahenk Z, Kissel JT, Mendell JR. Painful sensory neuropathy: Prospective evaluation using skin biopsy. Neurology. 1999; 53:1641–1647. [PubMed: 10563606]

Persohn E, Canta A, Schoepfer S, Traebert M, Mueller L, Gilardini A, Galbiati S, Nicolini G, Scuteri A, Lanzani F, Giussani G, Cavaletti G. Morphological and morphometric analysis of paclitaxel and docetaxel-induced peripheral neuropathy in rats. Eur. J. Cancer. 2005; 41:1460–1466. [PubMed: 15913989]

Peters CM, Jimenez-Andrade JM, Kuskowski MA, Ghilardi JR, Mantyh PW. An evolving cellular pathology occurs in dorsal root ganglia, peripheral nerve and spinal cord following intravenous administration of paclitaxel in the rat. Brain Res. 2007a; 1168:46–59. [PubMed: 17698044]

Peters CM, Jimenez-Andrade JM, Jonas BM, Sevcik MA, Koewler NJ, Ghilardi JR, Mantyh PW. Intravenous paclitaxel administration in the rat induces a peripheral sensory neuropathy characterized by macrophage infiltration and injury to sensory neurons and their supporting cells. Exp. Neurol. 2007b; 203:42–54. [PubMed: 17005179]

Polomano RC, Mannes AJ, Clark US, Bennett GJ. A painful peripheral neuropathy in the rat produced by the chemotherapeutic drug, paclitaxel. Pain. 2001; 94:293–304. [PubMed: 11731066]

Quasthoff S, Hartung HP. Chemotherapy-induced peripheral neuropathy. J. Neurol. 2002; 249:9–17. [PubMed: 11954874]

Raff MC, Whitmore AV, Finn JT. Axonal self-destruction and neurodegeneration. Science. 2002; 96:868–871. [PubMed: 11988563]

Ribeiro-da-Silva A, Kenigsberg RL, Cuello AC. Light and electron microscopic distribution of nerve growth factor receptor-like immunoreactivity in the skin of the rat lower lip. Neuroscience. 1991; 43:631–646. [PubMed: 1656323]

Sahenk Z, Barohn R, New P, Mendell JR. Taxol neuropathy. Electrodiagnostic and sural nerve biopsy findings. Arch. Neurol. 1994; 51:726–729. [PubMed: 7912506]

Siau C, Bennett GJ. Dysregulation of neuronal calcium homeostasis in chemotherapy-evoked painful peripheral neuropathy. Anesth. Analg. 2006; 102:1485–1490. [PubMed: 16632831]

Siau C, Xiao WH, Bennett GJ. Paclitaxel- and vincristine-evoked painful peripheral neuropathies: loss of epidermal innervation and activation of Langerhans cells. Exptl. Neurol. 2006; 201:507–514. [PubMed: 16797537]

Silva A, Wang Q, Wang M, Ravula SK, Glass JD. Evidence for direct axonal toxicity in vincristine neuropathy. J. Peripher. Nerv. Syst. 2006; 11:211–216. [PubMed: 16930282]

Sorrell JM, Caplan AI. Fibroblast heterogeneity: more than skin deep. J. Cell Sci. 2004; 117:667–675. [PubMed: 14754903]

Starkey ML, Davies M, Yip PK, Carter LM, Wong DJ, McMahon SB, Bradbury EJ. Expression of the regeneration-associated protein SPRR1A in primary sensory neurons and spinal cord of the adult mouse following peripheral and central injury. J. Comp. Neurol. 2009; 513:51–68. [PubMed: 19107756]

Tanner KD, Levine JD, Topp KS. Microtubule disorientation and axonal swelling in unmyelinated sensory axons during vincristine-induced painful neuropathy in rat. J. Comp. Neurol. 1998; 395:481–492. [PubMed: 9619501]

Topp KS, Tanner KD, Levine JD. Damage to the cytoskeleton of large diameter sensory neurons and myelinated axons in vincristine-induced painful peripheral neuropathy in the rat. J. Comp. Neurol. 2000; 424:563–576. [PubMed: 10931481]

Tsujino H, Kondo E, Fukuoka T, Dai Y, Tokunaga A, Miki K, Yonenobu K, Ochi T, Noguchi K. Activating transcription factor 3 (ATF3) induction by axotomy in sensory and motoneurons: A novel neuronal marker of nerve injury. Mol. Cell Neurosci. 2000; 15:170–182. [PubMed: 10673325]

Verzé L, Viglietti-Panzica C, Maurizo S, Sica M, Panzica G. Distribution of GAP-43 nerve fibers in the skin of the adult human hand. Anat. Rec. (A). 2003a; 272:467–473.

Verzé L, Viglietti-Panzica C, Panzica GC, Ramieri G. Expression of neuropeptides and Growth-Associated Protein 43 (GAP-43) in cutaneous and mucosal nerve structures of the adult rat lower lip after mental nerve section. Ann. Anat. 2003b; 185:35–44.

Verstappen CC, Heimans JJ, Hoekman K, Postma TJ. Neurotoxic complications of chemotherapy in patients with cancer: clinical signs and optimal management. Drugs. 2003; 63:1549–1563. [PubMed: 12887262]

Wallace VC, Blackbeard J, Segerdahl AR, Hasnie F, Pheby T, McMahon SB, Rice AS. Characterization of rodent models of HIV-gp120 and anti-retroviral-associated neuropathic pain. Brain. 2007; 130:2688–2702. [PubMed: 17761732]

Wang L, Hilliges M, Jernbert T, Wieglb-Edstrom D, Johansson O. Protein gene product 9.5-immunoreactive nerve fibres and cells in human skin. Cell Tiss. Res. 1990; 261:25–33.

Wang MS, Davis AA, Culver DG, Glass JD. *Wld*^{s} mice are resistant to paclitaxel (Taxol) neuropathy. Ann. Neurol. 2002; 52:442–447. [PubMed: 12325073]

Wendelschafer-Crabb G, Kennedy WR, Walk D. Morphological features of nerves in skin biopsies. J. Neurol. Sci. 2006; 242:15–21. [PubMed: 16448669]

Wiernik PH, Schwartz EL, Strauman JJ, Dutcher JP, Lipton RB, Paietta E. Phase I clinical and pharmacokinetic study of taxol. Cancer Res. 1987; 47:2486–2493. [PubMed: 2882837]

Wilkinson KD, Lee KM, Deshpande S, Duerksen-Hughes P, Boss JM, Pohl J. The neuron-specific protein PGP 9.5 is a ubiquitin carboxyl-terminal hydrolase. Science. 1989; 246:670–673. [PubMed: 2530630]

Windebank AJ, Grisold W. Chemotherapy-induced neuropathy. J. Peripher. Nerv. Syst. 2008; 13:27–46. [PubMed: 18346229]

Winklemann, RK. Cutaneous nerves. In: Zelickson, AS., editor. Ultrastructure of Normal and Abnormal Skin. Philadelphia: Lea & Febiger; 1967. p. 202-227.

Xiao WH, Bennett GJ. Chemotherapy-evoked neuropathic pain: Abnormal spontaneous discharge in A-fiber and C-fiber primary afferent neurons and its suppression by acetyl-L-carnitine. Pain. 2008; 144:714–720.

Xiao WH, Bennett GJ. Oxaliplatin-evoked painful peripheral neuropathy. 2010 Submitted.

Xiao WH, Bennett GJ, Bordet T, Pruss RM. Olesoxime (cholest-4-en-3-one, oxime): Analgesic and neuroprotective effects in a rat model of painful peripheral neuropathy produced by the chemotherapeutic agent, paclitaxel. Pain. 2009; 147:202–209. [PubMed: 19833436]

Zheng, H.; Xiao, WX.; Bennett, GJ. Mitotoxicity as the cause of the painful peripheral neuropathies evoked by the chemotherapeutics, paclitaxel and oxaliplatin. 13th World Congress on Pain. Montreal: IASP; 2010. Abstract # PW 097

Zimmermann M. Ethical guidelines for investigations of experimental pain in conscious animals. Pain. 1983; 16:109–110. [PubMed: 6877845]

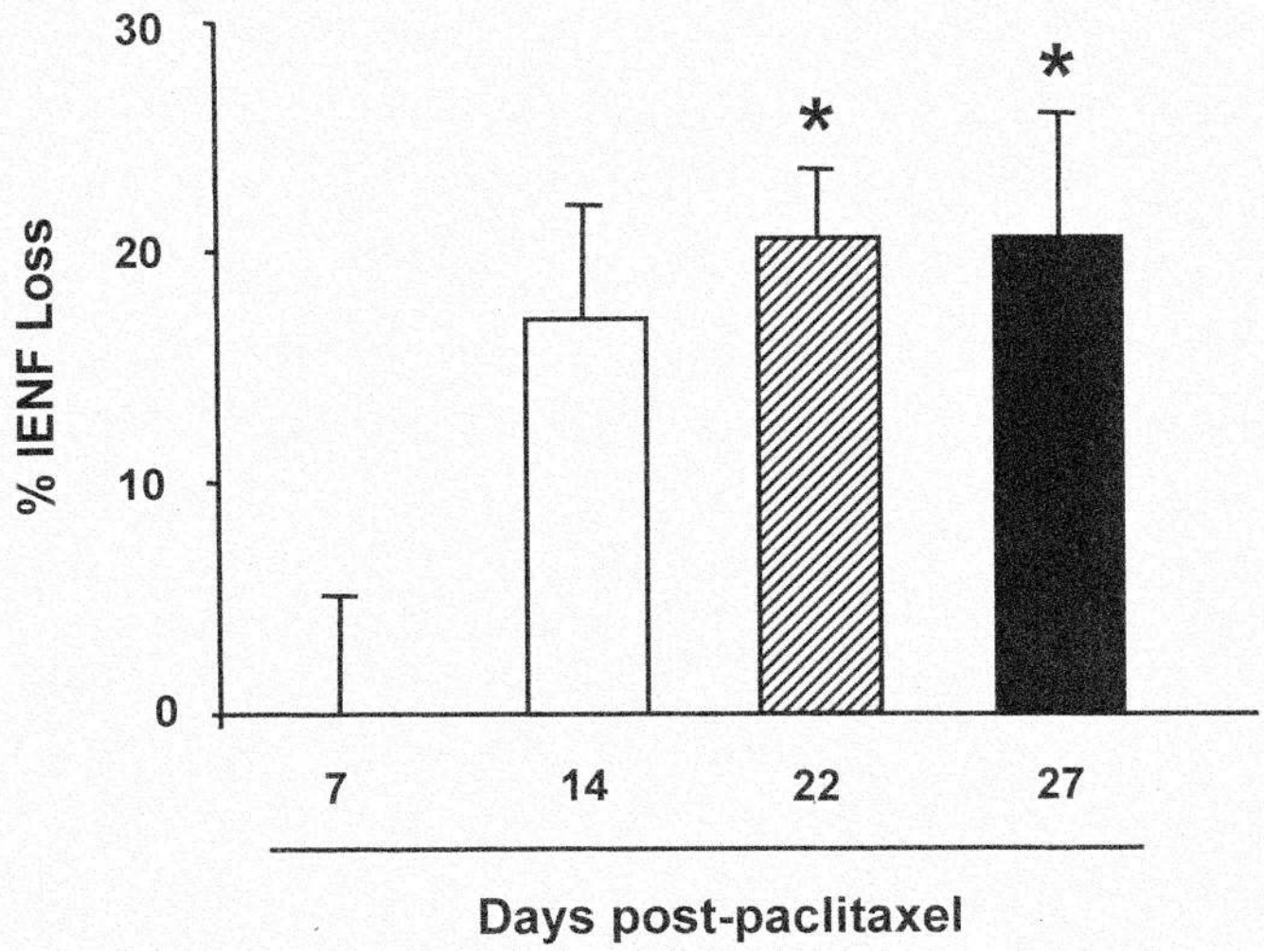

Fig. 1.

Time course of IENF loss in animals treated with our standard protocol (8 mg/kg total dose). There is no change in the mean number of IENFs per cm of epidermal border on D7, which is the day following the last injection of paclitaxel. A statistically non-significant decrease is seen on D14, which is the approximate time of onset for paclitaxel-evoked mechano-allodynia and mechano-hyperalgesia. Statistically significant IENF decreases are seen on D22 and D27 when mechano-allodynia and mechano-hyperalgesia are at peak, or near peak, severity. * $p < 0.05$ *vs.* control group.

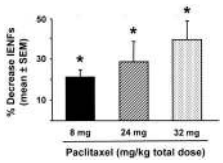

Fig. 2.

Effects of 8 mg/kg, 24 mg/kg, and 32 mg/kg paclitaxel on the number of IENFs per cm of epidermal border. The animals were sacrificed on D29-D36. For each dose the decrease is significant relative to their vehicle-matched control group. * $p < 0.05$.

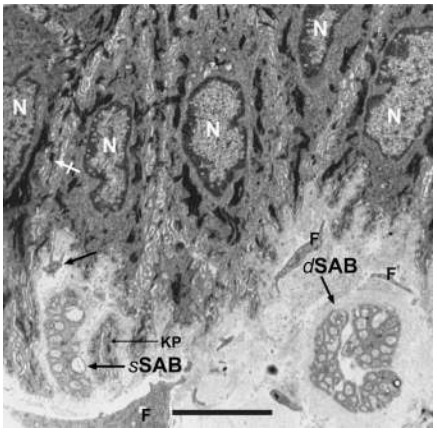

Fig. 3.

Superficial and deep subepidermal axon bundles (SAB). *s*SAB were found within indentations between adjacent basal keratinocytes. The crests of such indentations were located beneath the zipper-like junction between keratinocytes (barred white arrow). *d*SAB were found at or just below the papillary fibroblast level. Both types of SAB are composed of unmyelinated axons wrapped in the processes of a non-myelinating Schwann cell; there is no perineurium. *s*SAB were often associated with a cytoplasmic process (black arrow) that traveled towards the top of the indentation; we have not been able to identify these processes. F: fibroblast; N: Nuclei of basal keratinocytes; KP: keratinocyte process which in this section appears to be separate from its cell body. Scale bar: 5.0 μm. Image from a rat treated with a cumulative dose of 32 mg/kg paclitaxel.

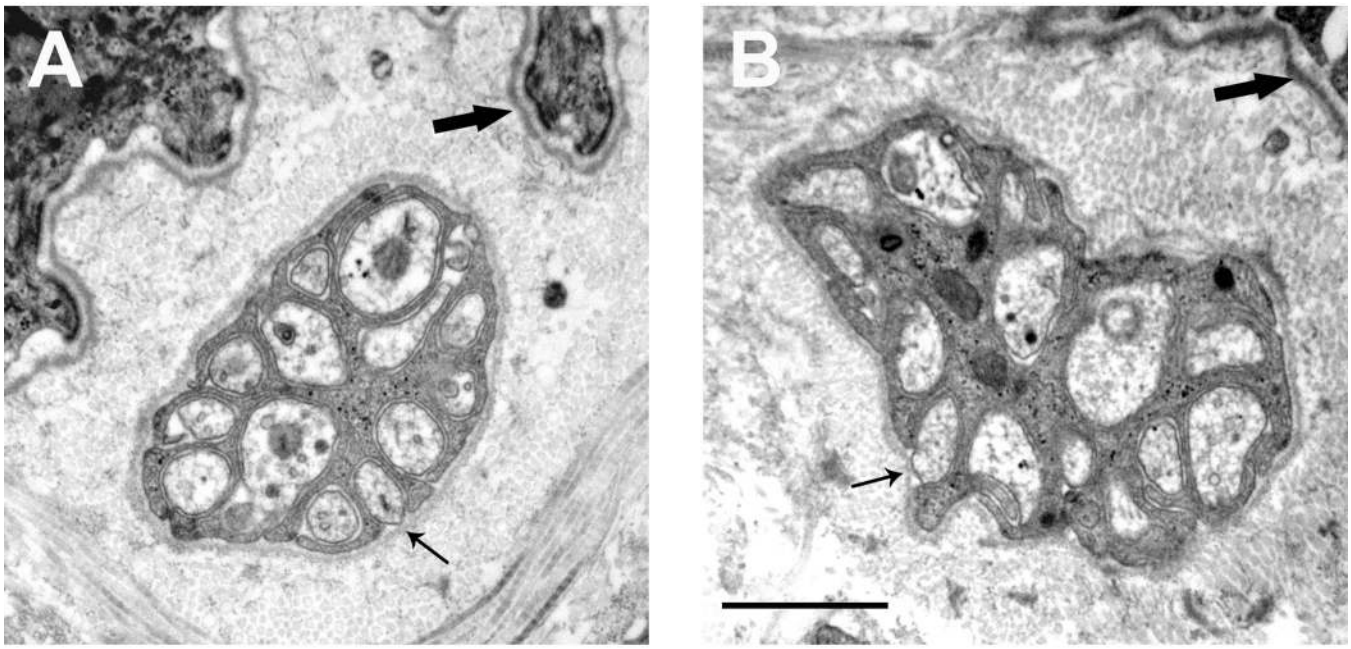

Fig. 4.

Details of *s*SAB from (A) a vehicle-injected control rat and (B) a rat treated with the highest dose of paclitaxel (4 × 8 mg/kg). In both control and paclitaxel-treated rats, *s*SAB axons had diameters ranging from 0.3 to 1.3 μm (mean 0.45 μm) and were always unmyelinated. The axoplasm was usually pale, and sometimes watery, with scarce microtubules and neurofilaments. Thick arrows point to the epidermal basal lamina; the thin arrows point to the Schwann cell's basal lamina. The axons below these arrows have widened mesaxons; presumably a preliminary step in the fiber leaving the bundle (see also Fig. 5C). Scale bar: 1.0 μm.

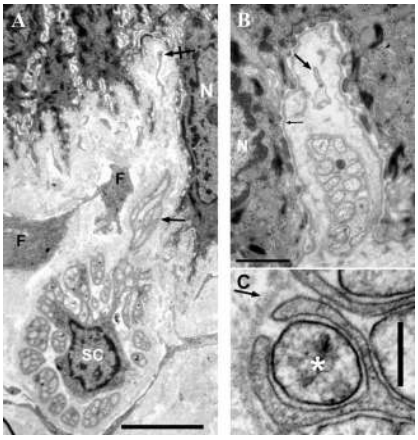

Fig. 5.

Details of subepidermal axon bundles (SAB). **A**: A presumed *d*SAB to *s*SAB transition. The *s*SAB axons (black arrow), which are sectioned tangentially in this view, have left the underlying *d*SAB and are traveling towards an indentation between adjacent keratinocytes. Barred black arrow: unidentified process; N: Nucleus of basal keratinocyte; F: fibroblast; SC: Schwann cell nucleus. **B**: An *s*SAB lying within an indentation between adjacent keratinocytes. Thin arrow: epidermal basal lamina. Thick arrow: unidentified process; N: Nucleus of basal keratinocyte. **C**: Axon (asterisk) lying along the margin of an *s*SAB with an expanded mesaxon. Arrow: Schwann cell basal lamina. Scale bars: (A) 5.0 μm; (B) 1.0 μm; (C) 0.25 μm. All images from vehicle-treated rats.

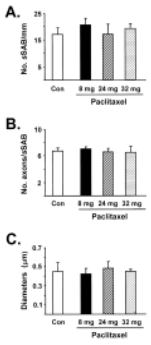

Fig. 6.

Superficial subepidermal axon bundle (*s*SAB) morphometry for vehicle-injected controls (Con) and rats receiving cumulative paclitaxel doses of 8, 24 and 32 mg/kg. **A**: Number of *s*SAB per mm of epidermal border. **B**: Number of axons per *s*SAB. **C**: Diameters of *s*SAB axons. Means ± SEM. There are no statistically significant differences between the control group and any of the paclitaxel dosage groups.

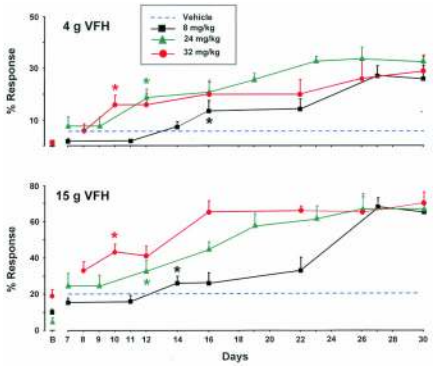

Fig. 7.

Time course of paclitaxel-evoked mechano-allodynia (responses to 4 g von Frey hairs; VFH) and mechano-hyperalgesia (responses to 15 g VFH). Vehicle or paclitaxel were given on D0, D2, D4 and D6. B: Pre-injection baseline response frequencies. The response frequencies and time course data from the group receiving our standard cumulative dose (8 mg/kg) of paclitaxel were nearly identical to what we have seen in our prior studies. Here we have combined the current and previous 8 mg/kg data into a large N composite (10–32 rats per time point). The responses of the vehicle-injected control rats did not vary significantly over time and were also nearly identical to what we have seen in our prior studies. Thus, here we also combine the data from the current control group and the control groups from prior studies into a large N composite (10–27 rats per time point) with the dashed lines showing the response frequencies averaged over all time points tested. Note that rats receiving 8 mg/kg paclitaxel have a notable delay between the last paclitaxel injection and the appearance of mechano-allodynia and mechano-hyperalgesia (coasting) and that this delay is shorter in rats receiving 24 mg/kg and shorter still in rats receiving 32 mg/kg. * $p < 0.05$ relative to own baseline (Dunnett's *t*-tests). Only the earliest day of significant mechano-allodynia or mechano-hyperalgesia is marked; in all cases, every day subsequent to the earliest significant time point was also significantly different from baseline with $p < 0.05$ or better.